Hindawi
Mathematical Problems in Engineering
Volume 2019, Article ID 2962154, 16 pages
https://doi.org/10.1155/2019/2962154

Research Article

Experiment and Numerical Simulation of the Dynamic Response of Bridges under Vibratory Compaction of Bridge Deck Asphalt Pavement

An-Ping Peng,[1] Han-Cheng Dan ,[1] and Dong Yang[2]

[1]*School of Civil Engineering, Central South University, Hunan, Changsha 410075, China*
[2]*School of Civil Engineering, Central South University, Changsha 410075, China*

Correspondence should be addressed to Han-Cheng Dan; danhancheng@csu.edu.cn

Received 26 February 2019; Revised 3 June 2019; Accepted 12 June 2019; Published 10 July 2019

Academic Editor: Gregory Chagnon

Vibratory compaction of bridge deck pavement impacts the structural integrity of bridges to certain degrees. In this study, we analyzed the dynamic response of different types of concrete-beam bridges (continuous beam and simply supported beam) with different cross-sectional designs (T-beam and hollow-slab beam) under vibratory compaction of bridge deck asphalt pavement. The dynamic response patterns of the dynamic deformation and acceleration of bridges under pavement compaction were obtained by performing a series of field experiments and a three-dimensional finite element simulation. Based on the finite element model, the dynamic responses of bridge structures with different spans and cross-sectional designs under different working conditions of vibratory compaction were analyzed. The use of different vibration parameters for different bridge structures was proposed to safeguard their structural safety and reliability.

1. Introduction

Bridge deck pavement is the protective layer paved over bridge deck slabs to prevent the direct wear of slabs by vehicle wheels, diffuse the load of vehicles, and provide a flat but skid-resistant surface for vehicles to drive on [1, 2]. There are several types of bridge deck pavement. Most express highway bridges are paved with asphalt mixture [3–5]. The performance of asphalt mixture-paved bridges is affected by the asphalt compaction quality. Poorly compacted asphalt pavements may suffer defects such as cracks, ruts, and water damage [6–8]. Such defects may compromise express highway performance and are a major cause of traffic accidents [9]. There are three primary methods of asphalt pavement compaction: static rolling, vibratory rolling, and oscillatory rolling. Whether vibratory rolling is appropriate for compacting bridge deck pavement is still a subject of dispute, as excessive vibratory loads may cause significant displacement in the bridge structure, thereby damaging it [10–12]. Vibratory compaction is not recommended, though not prohibited either, in the *Technical Specification for Construction of Highway Asphalt Pavements* [13]. The means of compaction recommended in the specification is oscillatory compaction. Undeniably, vibratory rollers cause more significant dynamic deformation than oscillatory and static rollers, particularly when operating at greater excitation forces. However, the development and application of the oscillatory roller are still in the exploratory stage, and the oscillatory roller is inferior to the vibratory roller in the effective depth of compaction and operational reliability. Therefore, vibratory rolling is a more popular technique (as indicated by the higher inventory of vibratory rollers kept by construction companies) for bridge deck pavement compaction.

Bridge deck pavement compaction is a dynamic process; the movement and compaction forces of a vibratory roller inevitably affect the bridge structure and the asphalt pavement. The vibratory roller moves on the bridge deck during the working process, so it can be regarded as a special moving load. Many scholars have carried out related research on the

dynamics of the bridge structure under the action of moving loads. For instance, Fryba [14] proposed an analytic solution for the case of a simply supported continuous beam with homogeneous cross-section under a moving load. Li et al. [15] investigated the dynamic performance of arch bridges constructed with concrete-filled strengthened steel tubes under the load of moving vehicles. Lee [16] studied the feasibility of detecting the structural degradation of highway bridges under vehicle excitation in the laboratory environment. In the study on the dynamic impact of the speed of a moving load on four-span continuous structures based on an experiment and a finite element simulation, Yang [17] found that constant decelerations affect the dynamic response of structures. In an investigation of the effect of the compaction efficiency and speed of the vibratory roller on the degree of compaction, due to the strong force between the roller compactor and the bridge structure during the pavement compaction process, the bridge structure will generate a greater dynamic response than the normal moving load, and response caused by the different types of the roller will be different, too. For the dynamic response of the bridge structure under different rolling methods, scholars have also carried out a lot of research. In an investigation of the impact of different means of compaction on the bridge deck slab vibration and bridge deck compaction quality, Hou [18] found that the disturbance of the bridge deck slab resulting from the excitation force of a roller is a major factor causing bridge vibration. Compared with oscillatory rolling, vibratory rolling uses much greater forces but has the advantages of significantly higher efficiency, higher degree of final compaction, and more extensive crushing of coarse aggregates. Yang [19] comparatively analyzed the impact of vibratory and oscillatory compaction on a bridge structure, by performing an experiment to compare the bridge structure vibration resulting from oscillatory and vibratory compaction. Based on quantitative measurement and comparison of the accelerations of continuous small-box beams paved using vibratory and oscillatory rollers, Liu [20] concluded that the vibration effect of an oscillatory roller on the bridge body is markedly smaller. Wang et al. [21] comparatively analyzed the dynamic response of a continuous beam bridge under static, vibratory, and oscillatory compaction by performing a field experiment of vibration acceleration (natural frequency), stress (strain), and displacement (deflection) based on control indicators for the effects of oscillatory compaction on bridge structure. Gunther [22] and Bild [23] calculated and analyzed the mechanical response of steel bridge deck pavement by using a finite element model, compared the computational results of the finite element model with testing data of bridge engineering projects, and assessed the factors affecting the service life of bridge deck pavement from different perspectives. Ying [24] suggested that the combination of vibratory compaction and rubber rolling can guarantee the construction quality of asphalt mixture pavement over cement-concrete bridge deck and prevent inadequate compaction. Wang et al. [25] performed a comprehensive analysis of the static and dynamic stresses in a bridge deck slab during bridge deck pavement construction and proposed a sustainable technique for bridge deck pavement construction.

The above studies analyzed the effect of the different means of compaction on bridge deck pavement and bridge structure from different perspectives, but they lack comparative and quantitative analyses of the dynamic response of different types of bridges under different working conditions of bridge deck pavement construction. In this study, the dynamic impact of vibratory rolling on the structure of bridges with different spans and cross-sectional designs under different rolling conditions was analyzed, by employing the finite element method and performing a series of field experiments.

2. The Experiment of the Vibratory Rolling of Bridge Deck Asphalt Pavement

2.1. Experimental Scheme. Most highway bridges in China are of two cross-sectional designs: slab beam and ribbed beam. Of these two cross-sectional designs, hollow-slab beam and T-beam are the most popular. Therefore, bridges with the cross-sectional designs of concrete hollow-slab beam and T-beam and the two most popular structural designs, namely, simply supported beams and continuous beams, were selected for the field experiment on bridge deck pavement.

The field experiment tested the accelerations and dynamic deflections of the bridges under bridge deck pavement construction using a vibration roller. The flexural deformation of the main beams of bridges is an indicator commonly used for monitoring the rigidity and operational health of large bridges; it is also a major indicator used for the acceptance inspection and evaluation of the service performance and safety of bridges. According to the *General Specification for Design of Highway Bridges and Culverts* [26], the maximum midspan vertical deflection of a reinforced-concrete bridge should not exceed 1/600 of its calculated span. The acceleration of bridge structures under a dynamic load is a major indicator of structural safety. Field measurement of bridge acceleration is a simple task, and the resulting data are reliable. Therefore, the field experiment focuses on monitoring the deflection and vibration acceleration of bridge structures.

The bridges selected for the experiment include a 50 m simply supported T-beam bridge, a 3 × 25 m continuous T-beam bridge, a 5 × 30 m continuous T-beam bridge, and a 3 × 20 m continuous hollow-slab beam bridge, which are shown in Figure 1.

The experiment measured the deflection of the bridges using displacement meter. Direct measurement of the structural deformation of the bridges is difficult, owing to their large clearance heights. The suspension method was adopted for structural displacement measurement as follows. One end of a steel wire was fixed to a point (the displacement of which was to be measured) in the bridge slab, and a weight was attached to the other end of the steel wire. Thereby, the displacement at the measurement point could be transmitted to the suspending end of the steel wire. A displacement meter was placed under the suspending weight, such that the sensor of the displacement meter was pressed against the bottom surface of the weight and the displacement detected by the

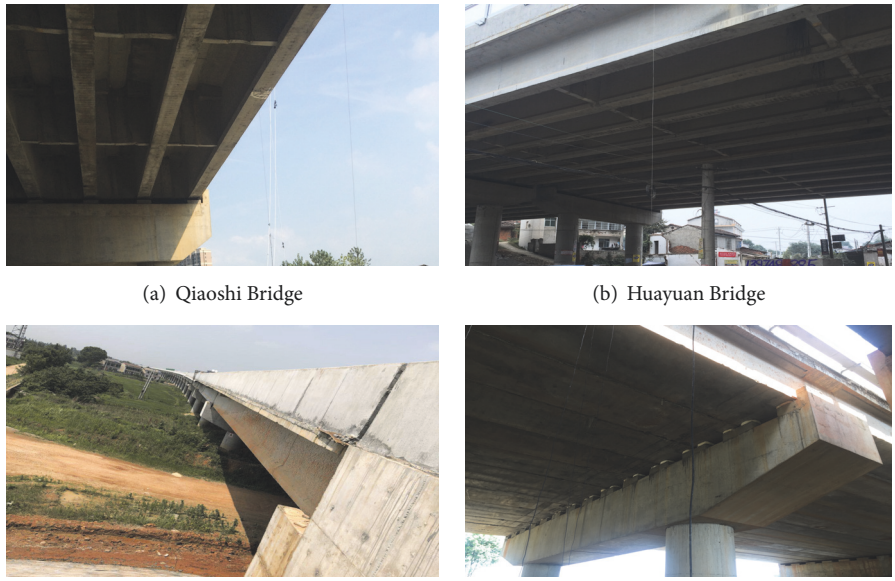

(a) Qiaoshi Bridge (b) Huayuan Bridge

(c) Daijiashan Bridge (d) Jintangping Bridge

Figure 1: Photos of test bridges ((a) Qiaoshi Bridge; (b) Huayuan Bridge; (c) Daijiashan Bridge; (d) Jintangping Bridge).

sensor was equal to the displacement in the slab, as shown in Figure 2(a). The structural acceleration of the bridges under bridge deck pavement construction was measured using a voltage-type acceleration sensor as follows. The target point for acceleration measurement was ground using sandpaper. The sensor was placed at the measurement point that has been ground smooth and fixed using epoxy resin, as shown in Figure 2(b). The lead of the sensor was connected to a signal acquisition system. The structural deflection and acceleration signals of the bridges under bridge deck pavement construction were acquired using a DH5922 test analysis system, as shown in Figure 2(c).

An edge beam was selected for the test. As the maximum deflection and dynamic response occur at the midspan of the structure, the sensors were placed at the midspan of the structures, such that the maximum dynamic response of the structure could be measured. Figure 3 shows the sensor configuration and measurement scheme for the field experiment.

In order to ensure that each test condition is constant, the type of paver, vibratory roller, and the working parameters of vibrating compactor were kept the same. Although some random loads (e.g., construction vehicle load) exist, the frequency of vibration in wavelet analysis result is almost the same. During the field experiment, concrete was paved using a 30-t VÖGELE paver, and the paved asphalt mixture was compacted using an HD130 vibratory double smooth drum roller (Hamm) and rolled using an XP302 pneumatic tire roller (XCMG). Figure 4 shows the pavement construction machinery configuration for the field experiment.

2.2. Experimental Results and Data Treatment. The dynamic response signals during the asphalt pavement compaction were collected using the DH5922 dynamic signal analysis system, with band-pass filtering applied to the initial dynamic signals using the system's built-in digital filter. Based on the working frequency of the vibratory roller used for the field experiment, clutter signals of frequencies lower than 35 Hz and higher than 55 Hz were filtered out. The resulting displacement and acceleration measurements were plotted as time-series curves. Figure 5 illustrates the signal acquisition and data treatment process.

The measurement of the dynamic response of the bridge structures under vibratory rolling includes the acceleration and deflection at the midspan of the bridge under vibration rolling. Figures 6 and 7 present the time-series curves of the deflection and acceleration, respectively, of the different bridge structures under vibratory rolling. The field measurements show that the maximum deflections of the bridges under vibratory rolling are smaller than L/600 and the peak values of the midspan accelerations of the bridge structures fall in the range of 5–10 m/s^2.

3. Finite Element Analysis of Vibratory Rolling

3.1. Theoretical Analysis of Vibratory Compaction

3.1.1. Dynamic Model of the Vibration System of Roller. A vibratory roller operates by generating vibration from a built-in vibrator in its rolling wheel. The vibration is transmitted to the rolling wheel and then acts on the material to be compacted.

The excitation force of the vibration drum comes from the centrifugal force resulting from the rotation of an eccentric block mounted in the vibration drum and driven by a motor through a drive shaft. The vibration is a result of the rotating eccentric block's natural tendency to maintain balance. This form of vibration is referred to as circular vibration. In

(a) Displacement meter (b) Vibration pickup (c) Signal sampling system

Figure 2: Sensors and signal acquisition devices for the field experiment.

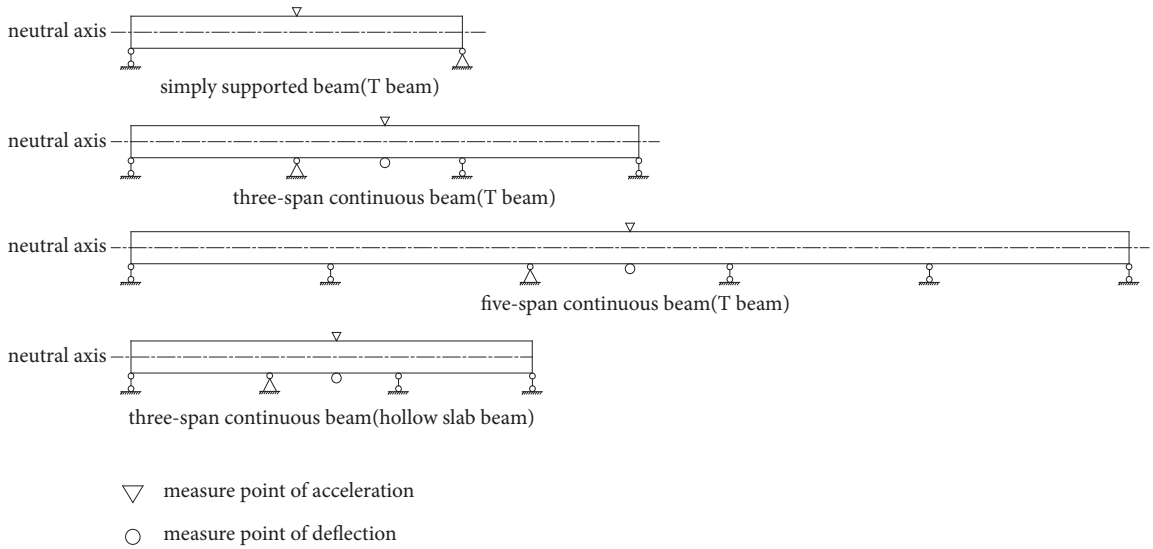

Figure 3: Measurement point configuration for the field experiment.

circular vibration, the direction of the excitation force is the same as that of the centrifugal force. The force resulting from the rotating eccentric block and acting from the vibratory drum on the ground varies periodically in a simple harmonic pattern. Figure 8 illustrates the principle underlying circular vibration.

Therefore, the vibration of the vibratory roller acting on the pavement can be simplified and simulated as a sine-wave load in the subsequent analysis and computation.

3.1.2. Analysis of the Dynamic Response Resulting from Bridge Deck Pavement Construction. The roller moves across the bridge deck to compact the bridge deck pavement. With the vibration effect of the roller neglected, the moving roller can be taken as a constant force moving across the bridge deck. Figure 9 illustrates the deflection response of the simply supported beam bridge and continuous beam bridge (three spans) under the impact of the moving roller, with its vibration effect neglected.

The deflection curves of the bridges under the moving load show that the maximum deflections occur near the midspan and the deflection curves of the bridges under the moving load can be taken as quasi-sine waves vibrating at certain frequencies around the corresponding static deflection curves. When the roller operates in its vibratory mode, the force that the vibration drum applies to the bridge structure has two components: the weight and the excitation force of the vibration drum. The deflection curve of the bridge structure under the drum exhibits a remarkable vibration effect and greater fluctuations.

The vibration effect can be measured using the dynamic amplification factor (μ), which is defined as the ratio of the maximum dynamic deflection of the bridge structure when its midspan is subjected to both the excitation force and weight of the vibratory roller and the maximum static deflection of the bridge structure when its midspan is subjected to the weight of the vibratory roller alone. The dynamic amplification coefficient is mathematically expressed as

$$\mu = \frac{y_{x=l/2}}{y_{st(x=l/2)}} \tag{1}$$

3.2. Finite Element Model of the Bridge Structure. A finite element analysis was performed for the QiaoShi Bridge,

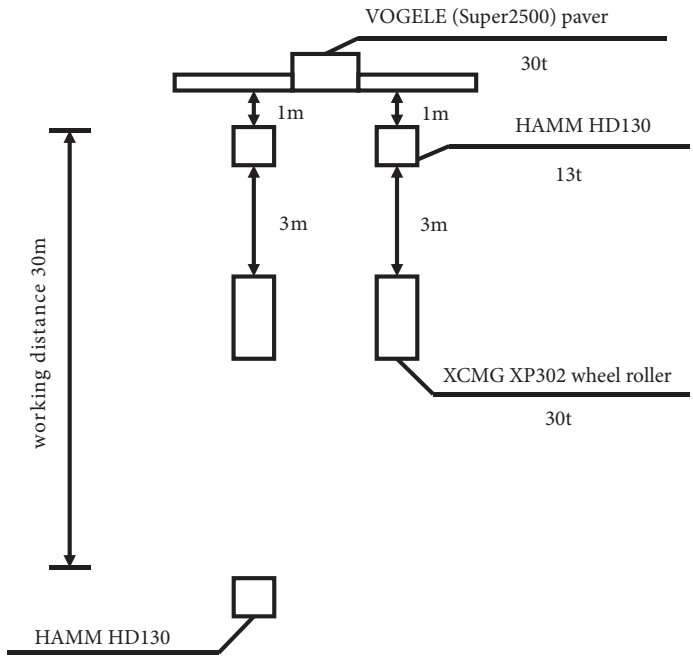

(a) Machine arrangement

(b) HAMM HD130 vibratory roller

(c) On site compaction

Figure 4: Scheme and configuration for the field experiment.

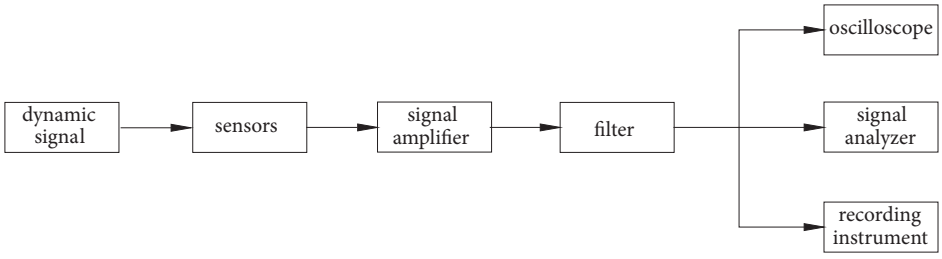

(a) Dynamic signal acquisition and processing

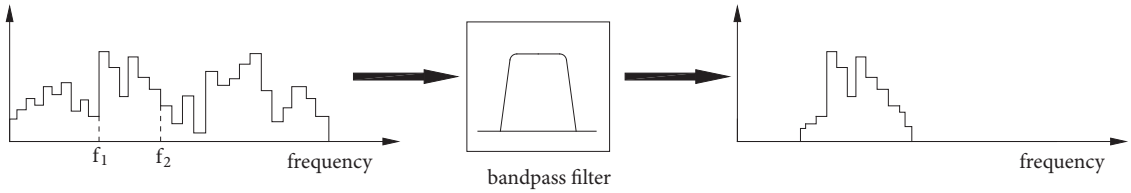

(b) Principle of bandpass filter

Figure 5: Dynamic signal acquisition and data treatment process using the DH5922 system.

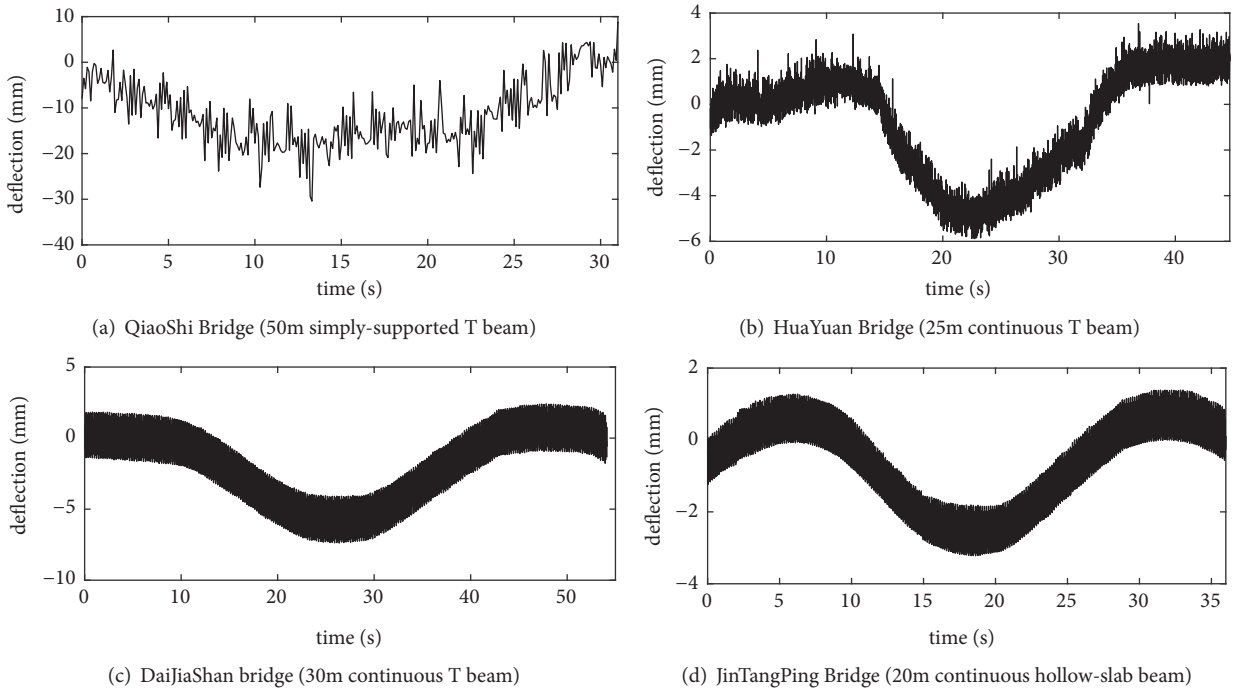

Figure 6: Time-series curves of field measurements of dynamic displacement.

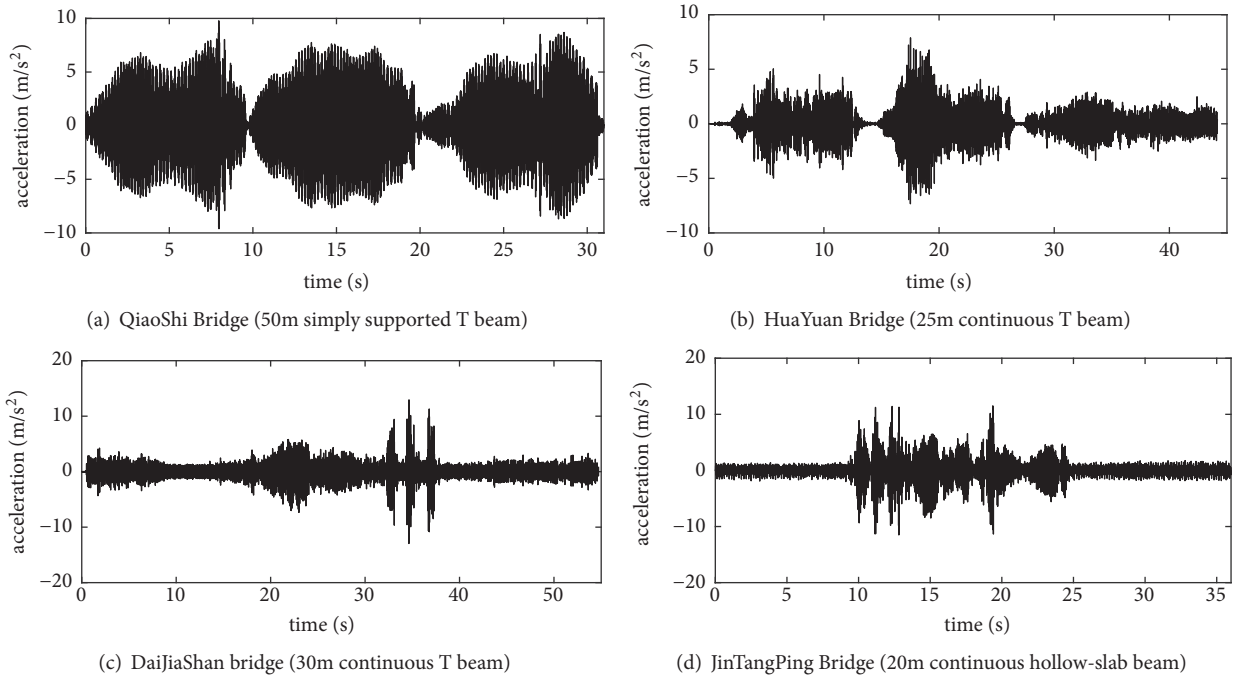

Figure 7: Time-series curves of field measurements of acceleration.

HuaYuan Bridge, DaiJiaShan Bridge, and the JinTangPing Bridge. Tables 1 and 2 present the structural parameters and material specifications, respectively, of the four bridges.

Finite element models were established for the bridges based on the structural parameters presented in Table 1. The models were developed in the ABAQUS environment, with their boundary conditions defined according to their structural designs (simply or continuously supported). Table 3 presents the parameters of the models of the bridge structures. Figure 10 presents the finite element model for the QiaoShi Bridge (simply supported T-beam structure) and JinTangPing Bridge (continuous hollow-slab beam structure).

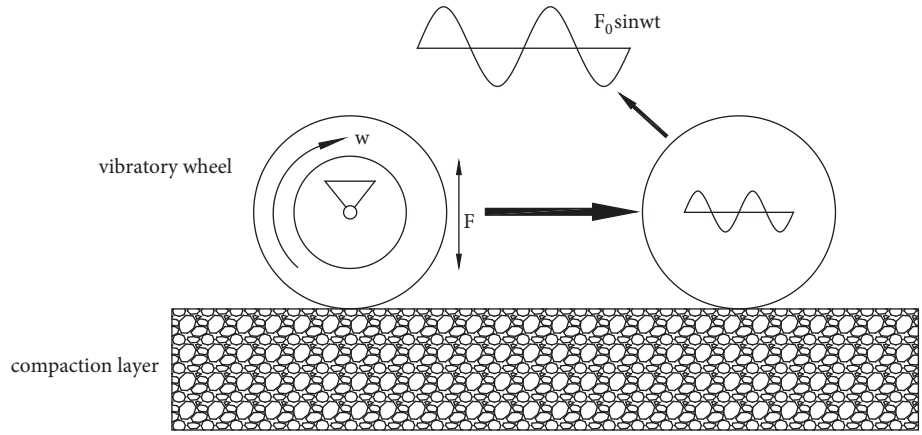

Figure 8: Illustration of circular vibration.

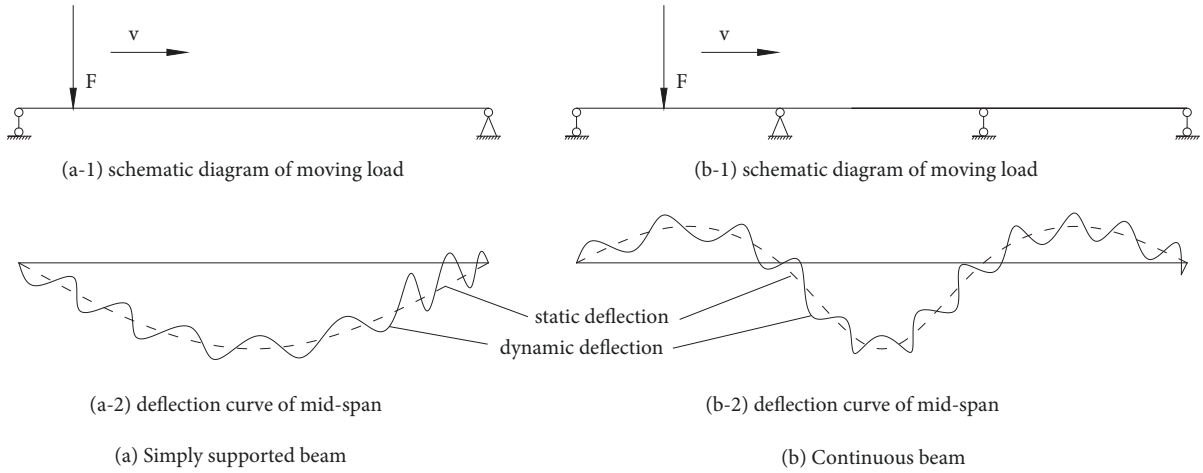

Figure 9: Deflection curves of structures under a moving load.

3.3. Vibration Load of Roller. Table 4 presents the working parameters of the HD130 double smooth drum vibratory roller.

The vibratory roller operates by vibrating its rear wheel while rolling on its front wheel. The vibration that the vibration wheel applies to the bridge structure is simple harmonic vibration, which can be expressed as a sine function as follows:

$$F = F_0 \sin \omega t \tag{2}$$

where F_0 is the excitation force generated by the roller and $F_0 = M_e\omega^2$, M_e is the eccentric moment of the eccentric block, and ω is the circular frequency of the sine function and $\omega = 2\pi f$.

In the numerical simulation, the force by which the roller acts on the bridge deck includes the weight of the vibration wheel and the excitation force generated by the simple harmonic vibration of the vibration wheel. Mathematically, this can be expressed as

$$P_1 = G + F_0 \sin \omega t \tag{3}$$

where G is the weight of the vibration wheel.

For an operating vibratory roller, the excitation force generated by its rotating vibration wheel (F_0) is usually greater than its weight, or even two or three times of its weight. While operating to compact the bridge deck pavement, the roller only acts as a pressure on the bridge deck. Thus, the excitation force applied by the vibrating roller on the bridge deck can be expressed as

$$P_1 = \begin{cases} G + F_0 \sin \omega t & P_1 > 0 \\ 0 & P_1 \le 0 \end{cases} \tag{4}$$

The action of the rolling wheel on the bridge structure can be taken as a moving constant force, which can be expressed as

$$P_2 = G \tag{5}$$

The load applied by the roller was taken as a pressure load. The resulting contact stress was computed according to the roller load distribution given by Zhi and Sha [27],

$$p = \frac{13P}{DL}, \tag{6}$$

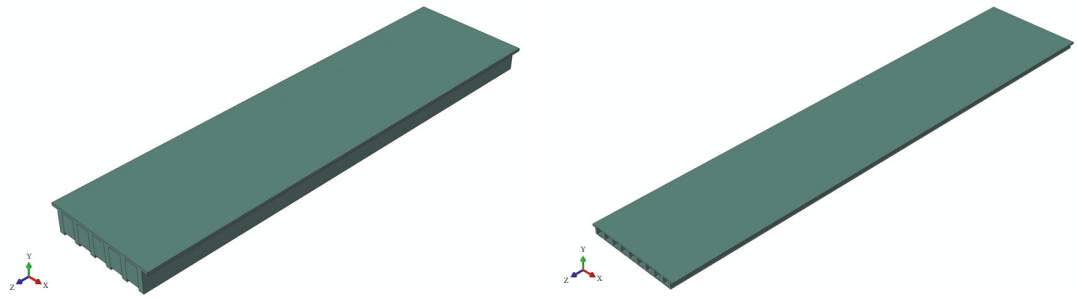

(a) QiaoShi Bridge (simply supported T beam) (b) JinTangPing Bridge (continuous hollow-slab beam)

Figure 10: Three-dimensional finite element models of the Qiaoshi Bridge and the Jintangping Bridge.

Table 1: Structural parameters of the bridge structures.

Structural Parameter	QiaoShi Bridge	HuaYuan Bridge	DaiJiaShan Bridge	JinTangPing Bridge
Cross-sectional design	T-beam	T-beam	T-beam	Hollow-slab beam
Structural design	Simply supported beam	Continuous beam	Continuous beam	Continuous beam
Bridge deck width (m)	12.9	12.9	16.8	16.25
Span (m)	50	3×25	5×30	3×20
Number of main beams	6	6	7	13
Beam width (m)	2.15	2.15	2.4	1.25
Height of main beams (m)	2.8	1.7	2	0.95

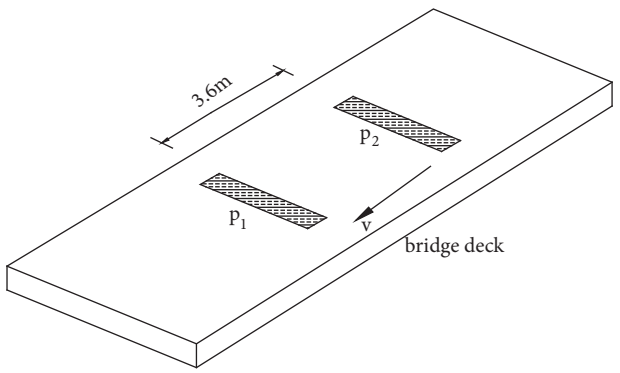

Figure 11: Illustration of the load of the roller.

Table 2: Concrete material specification.

Density (kg/m^3)	Modulus of elasticity (GPa)	Poisson ratio
2700	30	0.35

where D is the diameter of the rolling wheel and is equal to 1.2 m, and L is the width of the rolling wheel and is equal to 2.24 m.

Substituting (4) and (5) into (6), the following equations can be derived.

$$p_1 = \begin{cases} \dfrac{13\left(\mathrm{G} + F_0 \sin \omega t\right)}{DL} & p_1 > 0 \\ 0 & p_1 \le 0 \end{cases} \quad (7)$$

$$p_2 = \frac{13G}{DL} \quad (8)$$

For analyzing the stress in the bridge structure under the vibration load of the roller, the contact surface between the front/rear wheel of the roller and the bridge deck can be taken as a rectangular area, which was assumed to be 0.2 × 2 m (Figure 11).

The actual vibration frequency of the roller selected for bridge deck pavement construction during the field experiment was 40 Hz and an excitation force of 126 kN, and the working speed of the roller was 6 km/h. The above parametric values were used for the finite element computation. The load during vibratory rolling as expressed by (7) and (8) was computed by a user defined DLOAD subprogram in FORTRAN.

4. Results and Comparative Analysis

4.1. Computational Results. The midspan vertical deflection and acceleration of the bridge structures under a load with a vibration frequency of 40 Hz and an excitation force of 126 kN moving across the bridge deck at a speed of 6 km/h were simulated and computed. Figures 12 and 13 present the simulated time-series curves of the deflection and acceleration, respectively, of the four bridges under vibratory rolling. The computational results show that the maximum displacements of the bridge structures under the vibration of the roller are smaller than L/600, and the maximum and minimum deflection amplitudes of the bridges under vibration are 6.24 and 1.31 mm, respectively. The bridge structures experienced no deformation that threatened their structural safety.

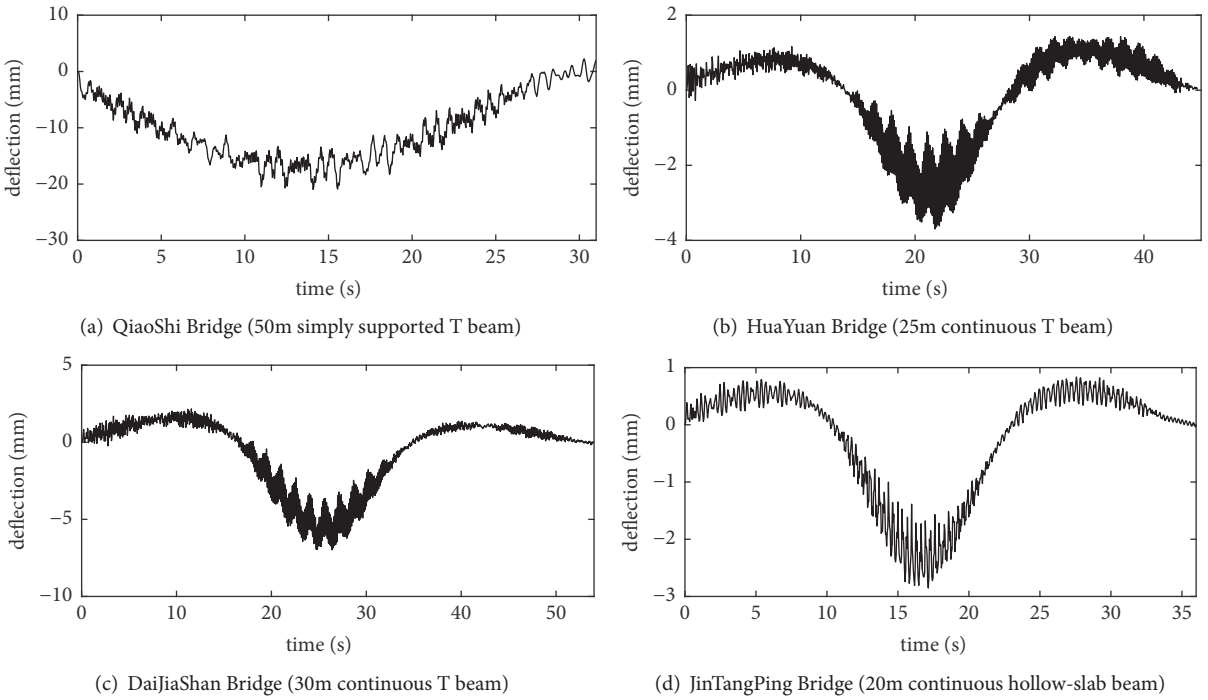

(a) QiaoShi Bridge (50m simply supported T beam)

(b) HuaYuan Bridge (25m continuous T beam)

(c) DaiJiaShan Bridge (30m continuous T beam)

(d) JinTangPing Bridge (20m continuous hollow-slab beam)

Figure 12: Computed time-series curves of the midspan deflection of the bridges.

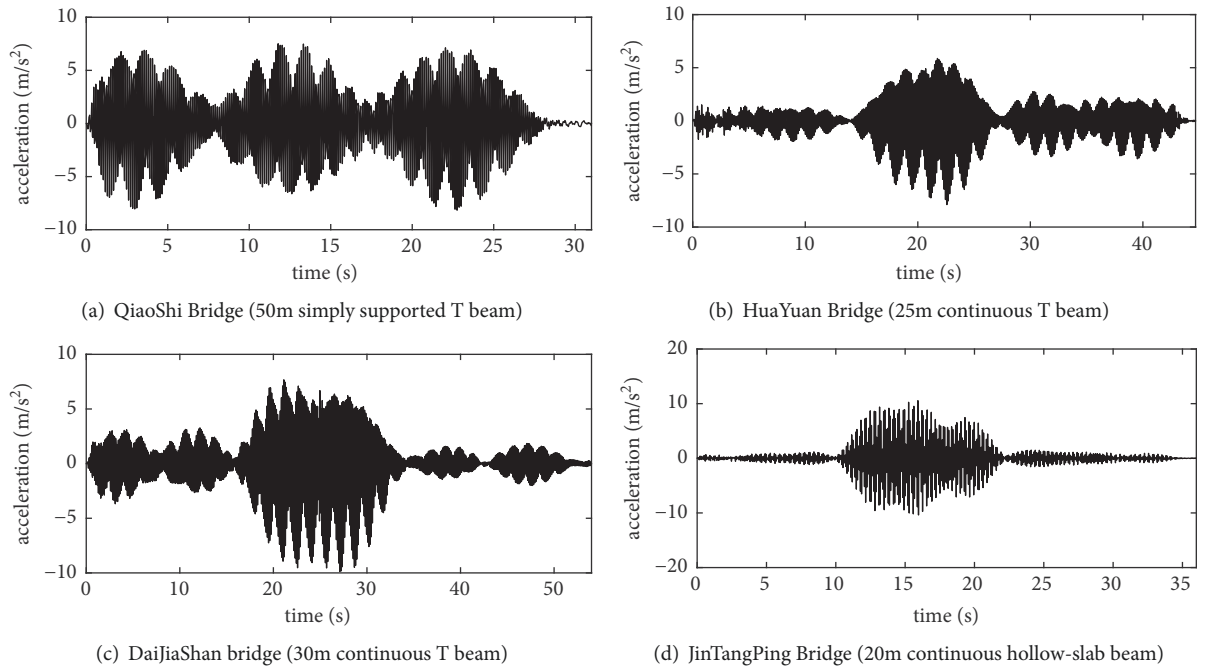

(a) QiaoShi Bridge (50m simply supported T beam)

(b) HuaYuan Bridge (25m continuous T beam)

(c) DaiJiaShan bridge (30m continuous T beam)

(d) JinTangPing Bridge (20m continuous hollow-slab beam)

Figure 13: Computed time series of the midspan acceleration of the bridges.

Table 3: Finite element models of the bridge structures.

Bridge name	QiaoShi Bridge	HuaYuan Bridge	DaiJiaShan Bridge	JinTangPing Bridge
Element type	C3D8R	C3D8R	C3D8R	C3D8R
Number of finite elements	91500	78000	156000	70200

Table 4: Working parameters of the vibratory roller.

Working weight (kg)	Weight of front/rear wheel (kg)	Wheel track (mm)	Working width (mm)	Vibration frequency (Hz)	Excitation force (kN)
13000	6500	3600	2240	42/50	139/194

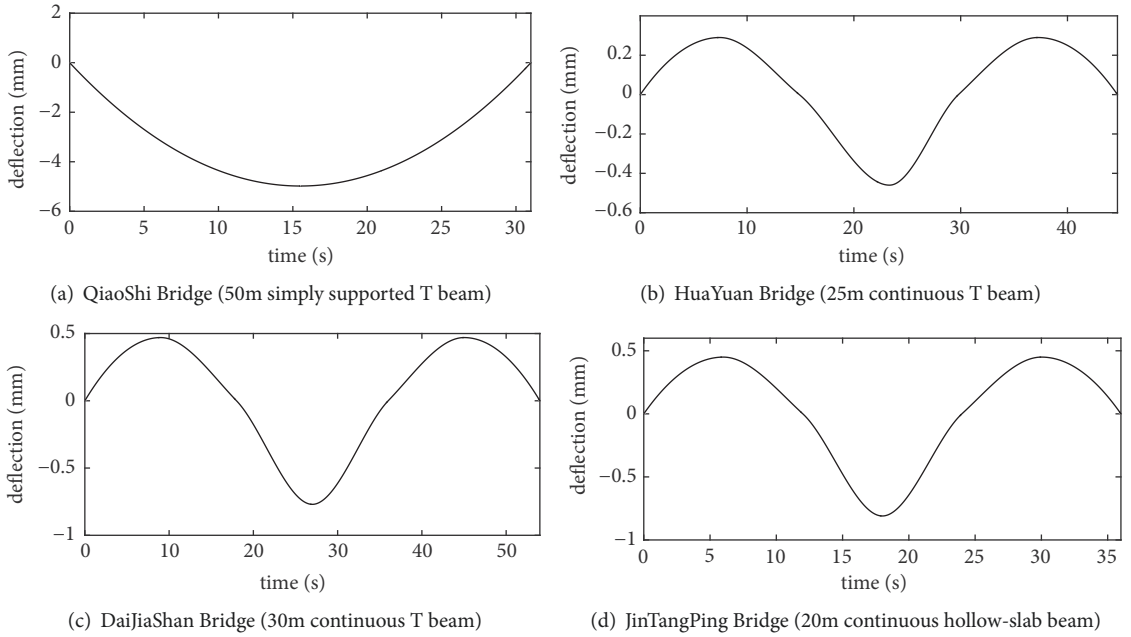

Figure 14: Deflection curves of the bridges under the load of the paver.

4.2. Comparison of Computational and Measurement Results. The midspan deflection obtained from the field experiment should be larger than that obtained from the numerical computation because the bridges were also subjected to the load of the paving machine in addition to the load of the roller during the field experiment. During the field experiment, the paving machine was placed at the very center of the bridge deck and moved very slowly. Thus, the load of the 30-t paver was assumed in the models as a static load acting on the different spans of the bridges. Figure 14 presents the curves of the deflection at the midspan of the bridge when the paver moved across the bridge deck. Then, the deflection measurements in Figure 6 minus the corresponding simulated deflections resulting from the load of the paver were compared with the computed deflections resulting from the load of the roller.

Figures 15 and 16 compare the measured and computed time-series curves of the four bridges under the load of the roller moving across the bridge deck at a speed of 6 km/h. The comparison reveals that the measured and computed time series of the midspan acceleration and deflection of the sample bridge structures under the vibration basically agree in terms of the peak value and variation trend, thereby confirming the reliability of the computational models.

There exist certain degrees of differences between the measurement and computational results, because the bridges were subjected to the loads of other construction machines (such as the pneumatic tire roller) in addition to the load of the vibratory roller and the several rollers operated in different irregular directions. This results in vibration loads of different magnitudes acting on the measurement points at different time points.

The comparison of the computational and measurement results reveals that the deflection of the bridge structures under the load of the vibratory roller during vibratory compaction of bridge deck pavement is within the limits provided in relevant specifications [26], and the computed and measured structural vibration accelerations agree well. Therefore, it is reasonable to conclude that bridge deck pavement compaction using vibratory roller does not affect the safety and reliability of the bridge structure, and vibratory compaction is a feasible option for bridge deck pavement construction.

5. Parameter Analysis and Discussion

5.1. Effect of Vibration Frequency on the Bridge Structure. An analysis shows that the vibration load of the vibratory roller is mainly determined by the working frequency of its vibration drum. Thus, the working frequency of the roller directly affects the reliability of the bridge structure and the compaction quality of asphalt pavement. The midspan deflections of the QiaoShi Bridge under vibration loads of different frequencies were computed. Table 5 presents the vibration parameters at different vibration frequencies.

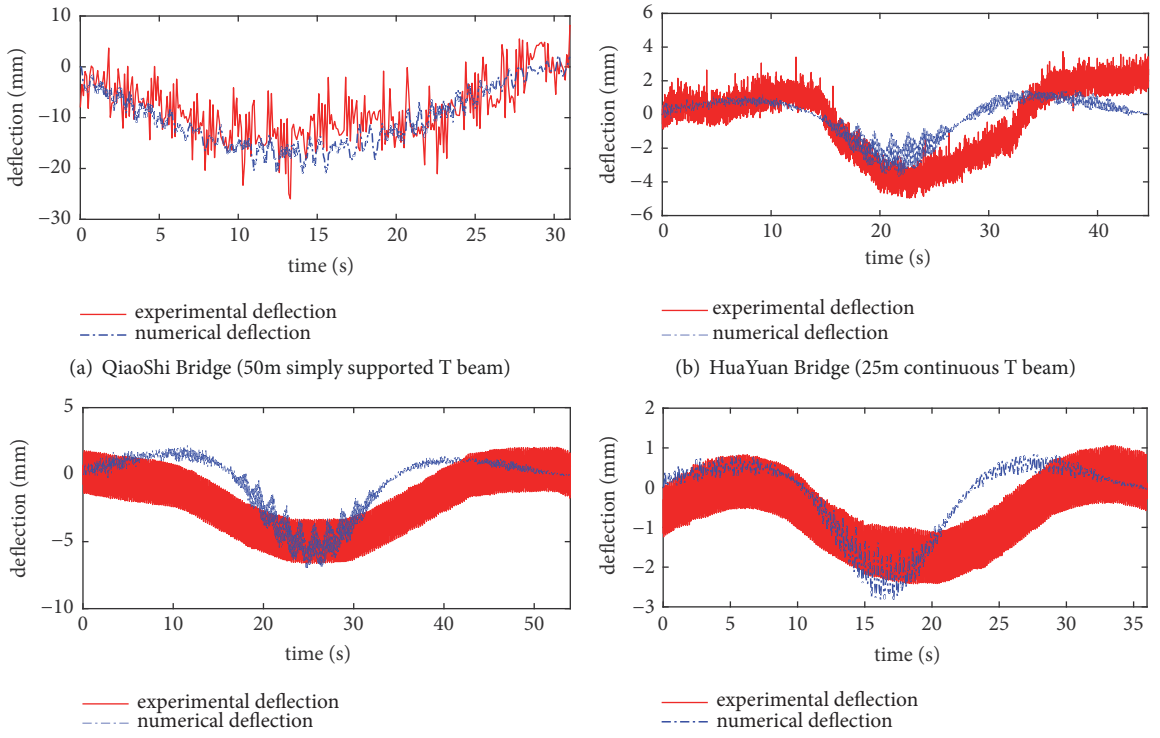

FIGURE 15: Comparison of computed and measured time-series curves of the deflection of the bridges.

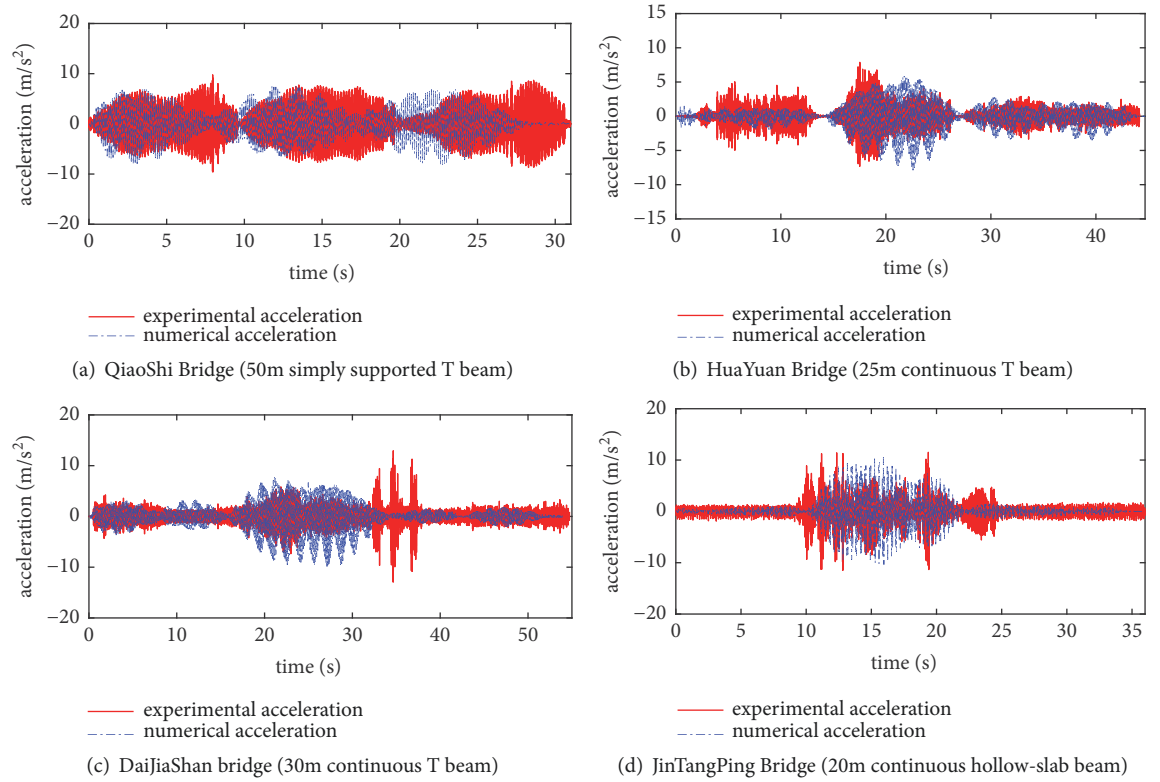

FIGURE 16: Comparison of computed and measured time-series curves of the acceleration of the bridges.

Table 5: Vibration loads at different vibration frequencies.

Working conditions	Vibration load parameters			
	Net weight of roller (kN)	Weight of front/rear wheel (kN)	Vibration frequency (Hz)	Excitation force (kN)
Working condition 1	130	65	0	0
Working condition 2	130	65	40	126
Working condition 3	130	65	50	197
Working condition 4	130	65	60	284

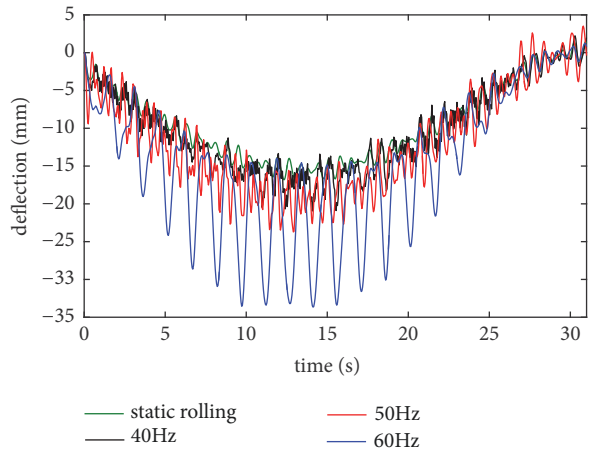

Figure 17: Time-series curves of midspan displacement at different frequencies.

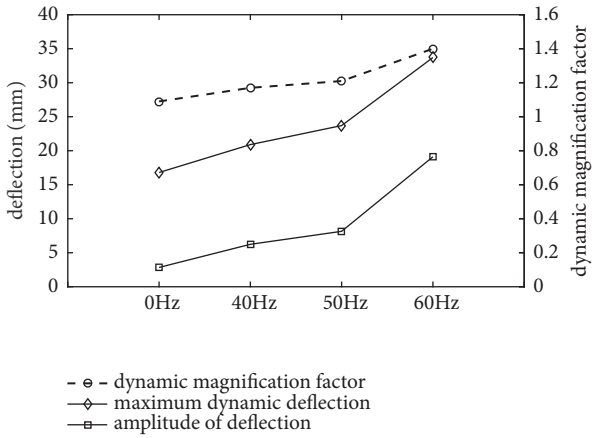

Figure 18: Deflection responses at different frequencies.

The computed midspan deflection resulting from the roller being statically placed at the midspan is 16.6 mm. Figures 17 and 18 present the time-series curves of the midspan deflection and the midspan deflection responses, respectively, of the QiaoShi Bridge under different working conditions. The computational results show that, at a frequency of 0 Hz (when the structure is subjected to a constant moving load that is equal to the weight of the roller), the maximum midspan deflection is 16.8 mm, the maximum midspan deflection amplitude is 2.84 mm, and the dynamic amplification factor of the dynamic load is 1.01. This indicates that, under the condition of static rolling, the maximum deflection approximates the static deflection and the structure generates insignificant vibration effect. When the roller operates in the vibratory rolling mode, the dynamic amplification factor gradually increases from 1.01 (the value under static rolling) to 2.03 as the vibration frequency of the roller increases, and the midspan deflection amplitudes at the three vibration frequencies of 40, 50, and 60 Hz are higher than the midspan deflection amplitude under static rolling, by 119.7%, 187.0%, and 572.9%, respectively. This indicates that the dynamic effect of structures subjected to vibration is a major factor affecting the structural safety, particularly at higher frequencies. Although the maximum midspan deflection of the bridges under high-frequency vibration is within the limit set in the specification, the dynamic effect resulting from the high-frequency vibration of roller may harm the bridge structures to certain degrees, particularly when several rollers operate simultaneously during bridge deck pavement construction or an asphalt mixture pavement is rolled multiple times to ensure adequate compaction. Therefore, the working frequency of a roller for pavement construction should be as low as possible; desirably, low-frequency vibration and static rolling are combined such that the structural integrity of the bridge can be safeguarded.

5.2. Effect of Rolling Speed on the Structure. The movement speed of a vibratory roller operating for bridge deck pavement construction is referred to as its working speed. The asphalt mixture compaction of bridge deck pavement construction is a three-stage process, preliminary compaction, repeat compaction, and final compaction. The roller working speeds for the three stages of compaction are 2–3, 5–6, and 8–9 km/h, respectively [28]. The midspan deflections of the QiaoShi Bridge during the three stages of compaction (preliminary compaction, repeat compaction, and final compaction at roller working speeds of 3, 6, and 8 km/h, respectively) at a roller vibration frequency of 40 Hz were analyzed. Figures 19 and 20 present the midspan displacement curves and deflection responses, respectively, at different working speeds of the roller.

The computational results show that both the maximum midspan deflection and deflection amplitude decrease with an increase in the working speed of the roller. At the same load frequency, the maximum deflection of the structure at a working speed of 3 km/h was 23.38 mm (which is translated to a dynamic amplification factor of 1.41) and was higher than that at a working speed of 6 km/h, by 11.9%. This is because, at a lower working speed, the roller takes a longer time to move

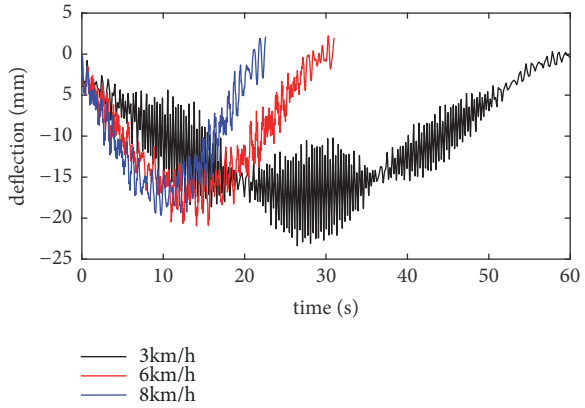

Figure 19: Midspan displacement variation curves at different working speeds of the roller.

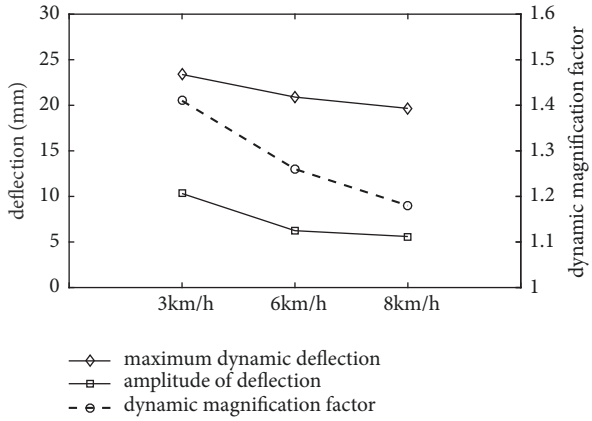

Figure 20: Deflection responses at different working speeds of the roller.

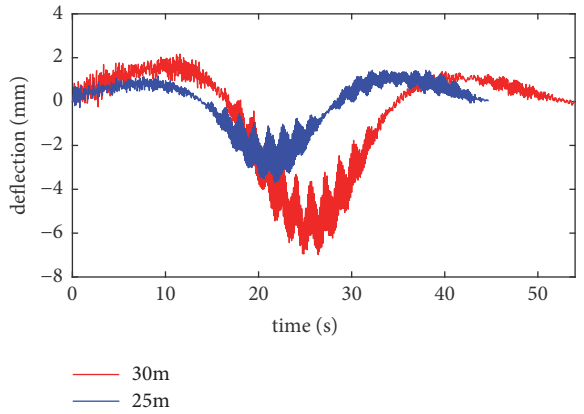

Figure 21: Midspan displacement variation curves of middle spans with different spans.

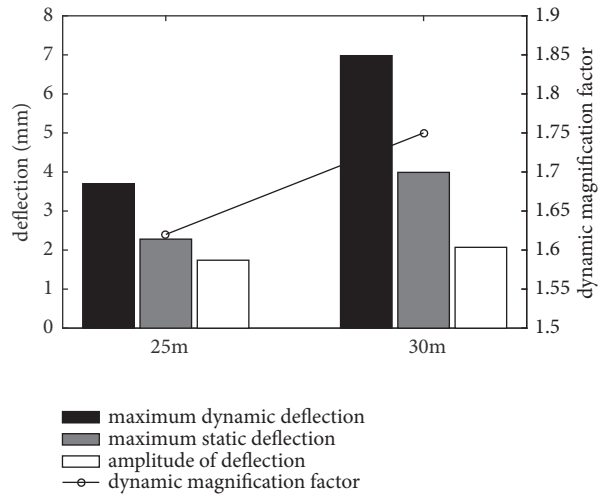

Figure 22: Deflection responses at different spans.

across the bridge structure. This results in a larger number of vibrations and a greater amount of energy generated by the roller during its movement across the bridge structure, thereby resulting in a larger dynamic response in the bridge structure [29]. However, the selection of the working speed of a vibratory roller is also determined by the desired degree of asphalt mixture pavement compaction. A higher roller working speed contributes to a smaller vibration effect on the bridge but may not facilitate the compaction of the asphalt mixture.

5.3. Effect of Bridge Span on the Structure. The bridges of different spans exhibit different dynamic responses under the same vibration load. Figure 21 compares the midspan time-series curves of the midspan displacement of the middle spans of the HuaYuan Bridge (3 × 25 m continuous T-beam bridge) and the DaiJiaShan Bridge (5 × 30 m continuous T-beam bridge). Figure 22 compares the dynamic displacement responses of the two bridges under the roller load.

The computational results show that, in the scenario where the roller moves across the midspan of the middle spans of the two bridges at a vibration frequency of 40 Hz, the maximum dynamic deflection of the structure with a span of 30 m is 6.98 mm and is higher than that of the structure with a span of 25 m. The value of deflection increases by 89%, and the deflection amplitude increases by 19%. This indicates that both the dynamic response of the structure under vibration rolling and the dynamics of the structure increase with an increase in the span. The midspan bending moment of a continuous structure subjected to a load acting at its midspan can be computed using the equation given by Lei [30]:

$$M_F = 0.203FL \tag{9}$$

According to (9), as the span of a continuous beam structure increases (with the same load acting on the structure), the bending moment of the structure increases and, thus, the midspan static deflection and dynamic deflection of the structure increase.

5.4. Effect of Cross-Sectional Design on the Structure. To investigate the different dynamic responses of bridge structures with different cross-sectional designs subjected to the vibration load of the roller, the displacement time-series curves of the HuaYuan Bridge and the JinTangPing Bridge

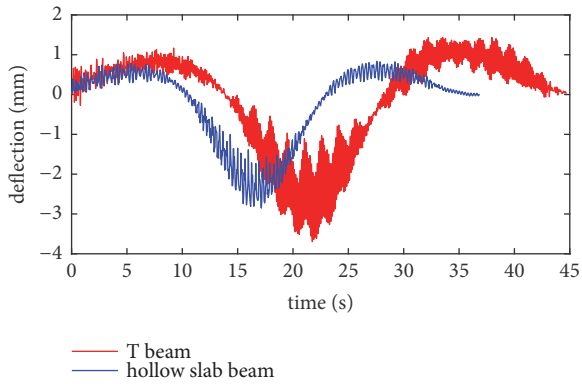

Figure 23: Time-series curves of the midspan deflections of the middle spans of bridges with different cross-sectional designs.

were compared, as shown in Figure 22, and their maximum midspan dynamic deflection-span ratios were computed, with the results shown in Figure 23. Figures 23 and 24 show that, at the same roller vibration load, the maximum dynamic deflections of the JinTangPing and HuaYuan Bridges are 2.85 and 3.70 mm, respectively; the maximum deflection amplitudes of the two bridges are 1.17 and 1.74 mm, respectively; and the maximum dynamic deflection-span ratio of the middle span of the JinTangPing Bridge is 1.43×10^{-4} and is smaller than that of the HuaYuan Bridge, by 3.4%.

The cross-sectional design of the JinTangPing Bridge is a hollow-slab beam, while that of the HuaYuan Bridge is T-beam. Compared with a T-beam bridge, a hollow-slab beam bridge (under the same load) has a larger cross-sectional area (consisting of the cross-sectional areas of the top and bottom plates) and, thus, has a greater capacity to resist the positive and negative bending moment. And the negative bending moments at the supports facilitate the effective release of the midspan bending moment. At a given cross-sectional area, a hollow-slab beam has a greater bending moment of inertia and a greater torsional rigidity than a T-beam bridge and, thus, exhibits a smaller dynamic response than the T-beam bridge under the same roller vibration.

5.5. Dynamic Response at Different Positions of Bridge Span. Due to the constraint effect near the bridge fulcrum, the position far from the fulcrum is more likely to exhibit larger deformation. In order to quantitatively analyze the dynamic deflection at different positions, the dynamic response at the fulcrum, 1/8L, 1/4L, 3/8L, and 1/2L, is calculated and shown in Figure 25. The maximum dynamic deflection and dynamic deflection amplitude gradually increase and basically have a linear trend from fulcrum to the middle of the span. The maximum dynamic deflection at each location competing with the fulcrum increases by 88%, 275%, 344%, and 414%, respectively, and the dynamic deflection amplitude increases by 28%. 57%, 70%, and 110%, respectively. Under the constant roller load, the dynamic response of the bridge structure at the mid-span position is far greater than that near the fulcrum. Large deflection means more energy dissipation in compaction process. It can be inferred that the compaction energy or compaction work by vibratory roller to the materials of bridge deck pavement is relatively lower than that at fulcrum. Therefore, it can be suggested that the parameter of vibration frequency or rolling speed may be adjusted to adapt this situation by taking the compaction degree into account. For instance, higher vibration frequency and lower rolling speed can be adopted at the middle span of bridge, and more compaction work can be done to the asphalt pavement. On the contrary, the relatively lower vibration frequency and higher rolling speed is applied for the location of fulcrum.

6. Conclusion

In this study, the dynamic responses of bridges with different structures, spans, and cross-sectional designs during bridge deck pavement construction using vibratory roller were investigated and analyzed, by performing a series of field experiments and finite element numerical simulations. Our conclusions can be summarized as follows.

(1) The dynamic responses of the bridge structures under different working conditions were simulated, using the finite element method. The resulting dynamic flexural deformations and dynamic accelerations of different types of bridges with different cross-sectional designs were compared with the results of the field experiment. The simulation and experimental results agree well, thereby confirming the validity of the model.

(2) The results of field test and finite element analysis show that during the pavement construction process, the maximum dynamic deflection of the bridge structure grows up with the increase of the vibration frequency which is in the normal working frequency range of the vibratory roller. For the simply supported beam, the dynamic deflection at high frequencies is 13% higher than that at low frequencies. As the frequency is further increased to 60 Hz, although the deflection of the bridge structure does not exceed the allowable value, the amplitude of the deflection is far greater than that under the rated frequency. Therefore, it is not advisable to use a higher frequency roller (high frequencies can provide greater excitation force to improve high compaction degree of asphalt pavement) during the construction process to ensure structural safety.

(3) The working speed of the vibratory roller is an important factor affecting the structural dynamic response. The working speed corresponding to different rolling stages makes the maximum dynamic magnification factor of the bridge different by more than 10%. Therefore the selection of the mode of rolling for bridge deck pavement construction should be based on the stage of rolling and the working speed for a specific stage of rolling. It is recommended that static rolling be used for the preliminary stage of rolling and vibratory rolling for the subsequent stages in order to ensure both compaction quality of asphalt pavement and the structural integrity of the bridge.

(4) The dynamic response of the bridge under vibratory load increases with an increase in the span. Thus, for bridge deck pavement construction of large-span bridge structures, smaller roller vibration frequencies are recommended to

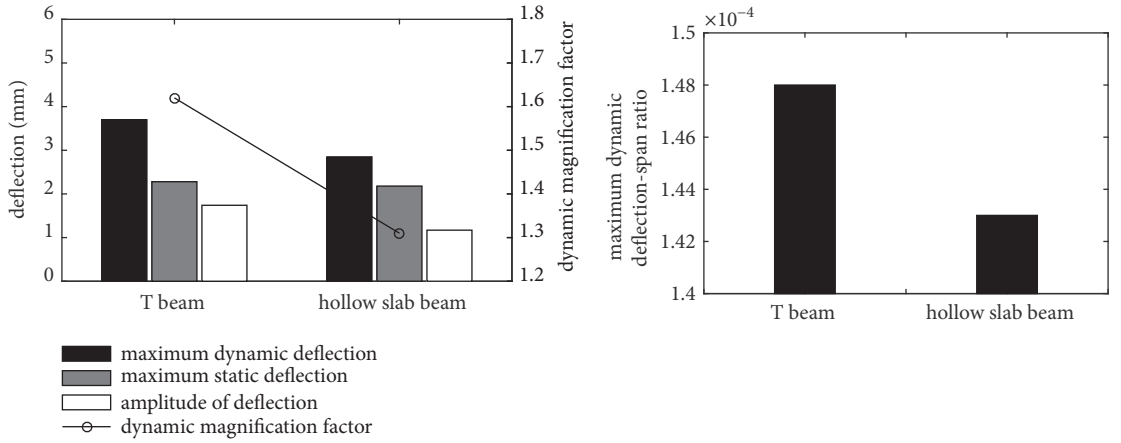

(a) Deflection response at different section types

(b) Maximum dynamic deflection-span ratio at different section types

Figure 24: Deflection responses of bridges with different cross-sectional designs.

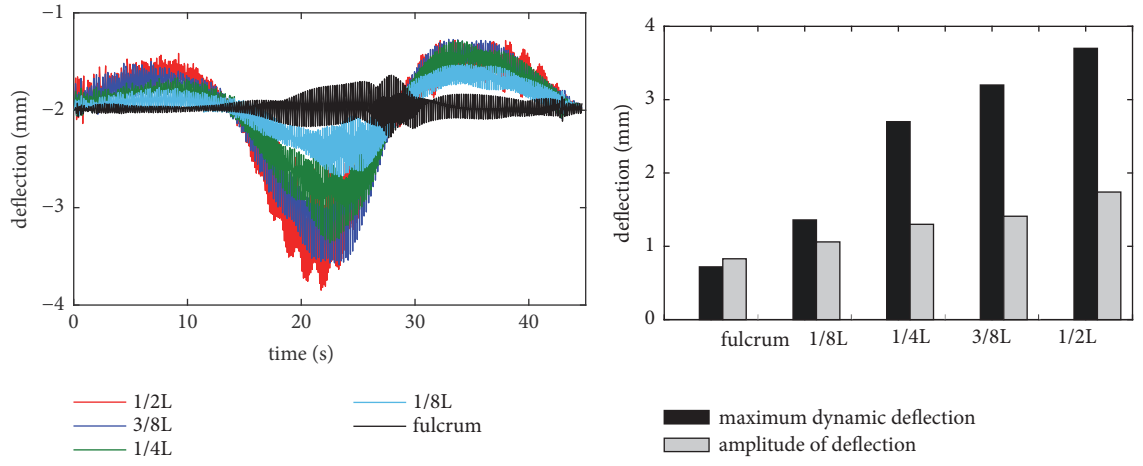

(a) Deflection curve at different positions

(b) Deflection response at different positions

Figure 25: Deflection curves at different positions (L is the length of bridge span).

reduce the vibration load applied by the roller on the bridge structure and to prevent the bridge structure from excessive deformation. Bridges with different cross-sectional designs exhibit different dynamic responses during bridge deck pavement construction. For hollow-slab-beam and box-beam bridges, the dynamic deflection under the same roller load is reduced by about 4% compared with the T-beam bridge under the same span. Thus, higher roller vibration frequencies are recommended to achieve better compaction, whereas for T-beam bridges, it is recommended that the working frequency of the roller be controlled below the rated frequency while increasing the number of rolling operations to achieve the desired degree of asphalt pavement compaction.

(5) For the bridge structure, there is an obvious difference in the dynamic response at different positions. The deflection and vibration amplitude of the mid-span under the impact of the roller may be several times higher than the fulcrum position. Therefore, during the construction process, when the road roller travels to different positions of the bridge span, the rolling speed and frequency should be appropriately adjusted accordingly. For instance, higher vibration frequency and lower rolling speed can be adopted at the middle span of bridge, and more compaction work can be done to the asphalt pavement. On the contrary, the relatively lower vibration frequency and higher rolling speed are applied for the location of fulcrum.

Data Availability

The data used to support the findings of this study are included within the article.

Conflicts of Interest

The authors declare that they have no conflicts of interest.

Acknowledgments

This research was supported by the National Natural Science Foundation (Grant No. 51308554), the Guizhou Transportation Science and Technology Foundation (Grant No. 2013-121-013; Grant No. 2019-122-006), and the Hunan Transportation Science and Technology Foundation (Grant No. 201622) to the first author.

References

[1] C. Cui, Q. Zhang, H. Hao, J. Li, and Y. Bu, "Influence of asphalt pavement conditions on fatigue damage of orthotropic steel decks: parametric analysis," *Journal of Bridge Engineering*, vol. 23, no. 12, Article ID 04018093, 2018.

[2] G. P. Zhou, A. Q. Li, J. H. Li, and M. J. Duan, "Test and numerical investigations on static and dynamic characteristics of extra-wide concrete self-anchored suspension bridge under vehicle loads," *Journal of Central South University*, vol. 24, no. 10, pp. 2382–2395, 2017.

[3] K. Zhang and Y. F. Luo, "Interlaminar performance of waterproof and cohesive materials for concrete bridge deck under specific test conditions," *Journal of Materials in Civil Engineering*, vol. 30, no. 8, Article ID 04018161, 2018.

[4] H. C. Dan, J. W. Tan, and J. Q. Chen, "Temperature distribution of asphalt bridge deck pavement with groundwater circulation temperature control system under high- and low-temperature conditions," *Road Materials and Pavement Design*, vol. 20, no. 3, pp. 509–527, 2019.

[5] H. C. Dan, Z. Zhang, J. Q. Chen, and H. Wang, "Numerical simulation of an indirect tensile test for asphalt mixtures using discrete element method software," *Journal of Materials in Civil Engineering*, vol. 30, no. 5, Article ID 04018067, 2018.

[6] Y. C. Li, S. Li, R. Lv et al., "Research on failure mode and mechanism of different types of waterproof adhesive materials for bridge deck," *International Journal of Pavement Engineering*, vol. 16, no. 7, pp. 602–608, 2015.

[7] H. Ma, Z. Zhang, B. Ding, and X. Tu, "Investigation on the adhesive characteristics of Engineered Cementitious Composites (ECC) to steel bridge deck," *Construction and Building Materials*, vol. 191, pp. 679–691, 2018.

[8] H. C. Dan, Z. Zhang, X. Liu, and J. Q. Chen, "Transient unsaturated flow in the drainage layer of a highway: solution and drainage performance," *Road Materials and Pavement Design*, vol. 20, no. 3, pp. 528–553, 2019.

[9] Y. L. Luo, "The technology for construction quality control of bridge deck pavement on yellow river 2nd bridge in Zhengzhou," *Applied Mechanics and Materials*, vol. 204-208, pp. 1967–1970, 2012.

[10] S. T. Wu, P. M. Huang, and J. Wang, "Analysis on analogue simulation for oscillatory compaction implementation in bridge deck pavement," *Applied Mechanics and Materials*, vol. 488-489, pp. 433–436, 2014.

[11] X. Z. Mao, *Research on the Influence of Oscillating Compaction on Bridge Structure [Ph. D thesis]*, Chang'an University, 2012.

[12] H. C. Dan, L. H. He, and L. H. Zhao, "Experimental investigation on the resilient response of unbound graded aggregate materials by using large-scale dynamic triaxial tests," *Road Materials and Pavement Design*, 2018.

[13] Research Institute of Highway Ministry of Transport, *Technical Specifications for Construction of Highway Asphalt Pavement*, Traffic Publishing House, 2004.

[14] L. Frýba, *Vibration of Solids and Structures under Moving Loads*, vol. 1, Springer, Dordrecht, Netherlands, 1972.

[15] Y. Li, L. H. Qin, Z. Li, and T. T. Yang, "Dynamic performance of strengthened concrete-filled steel tubular arch bridge due to moving vehicles," *Journal of Aerospace Engineering*, vol. 32, no. 1, Article ID 04018113, 2019.

[16] J. W. Lee, J. D. Kim, and C. B. Yun, "Health-monitoring method for bridges under ordinary traffic loadings," *Journal of Sound & Vibration*, vol. 257, no. 2, pp. 247–264, 2002.

[17] J. Yang, H. Ouyang, D. Stancioiu, S. Cao, and X. He, "Dynamic responses of a four-span continuous plate structure subjected to moving cars with time-varying speeds," *Journal of Vibration and Acoustics-transactions of the ASME*, vol. 140, no. 6, Article ID 061002, 2018.

[18] J. R. Hou and L. J. Zhao, "Effect of different compaction methods on bridge pavement," *Advanced Materials Research*, vol. 671-674, pp. 1073–1077, 2013.

[19] D. L. Yang, B. Chen et al., "Study on the influence of oscillating compaction on bridge structures," *Road Machinery & Construction Mechanization*, vol. 22, no. 6, pp. 48–50, 2005.

[20] P. Liu and G. C. Tian, "Research on vibration acceleration of asphalt concrete pavement of continuous small box girder," *Journal of Hebei Jiaotong Vocational and Technical College*, no. 2, pp. 35–39, 2009.

[21] J. Wang, L. J. Shi, and B. X. Zhang, "Experimental study on the influence degree of vibration and oscillatory compaction on bridge structure," *Jiangxi Building Materials*, no. 1, p. 141, 2014.

[22] G. H. Günther, S. Bild, and G. Sedlacek, "Durability of asphaltic pavements on orthotropic decks of steel bridges," *Journal of Constructional Steel Research*, vol. 7, no. 2, pp. 85–106, 1987.

[23] S. Bild, "Durability design criteria for bituminous pavements on orthotropic steel bridge decks," *Canadian Journal of Civil Engineering*, vol. 14, no. 1, pp. 41–48, 1987.

[24] X. M. Ying, D. F. Zhang, Q. Y. Li, and L. C. Meng, "Research on cement concrete bridge asphalt pavement compaction technology," *Key Engineering Materials*, vol. 599, pp. 224–229, 2014.

[25] L. B. Wang, Y. Hou, L. Zhang, and G. Liu, "A combined static-and-dynamics mechanics analysis on the bridge deck pavement," *Journal of Cleaner Production*, vol. 166, pp. 209–220, 2017.

[26] CCCC Highway Consultants, *General Specifications for Design of Highway Bridges and Culverts*, People's Communications Press Co., Ltd, 2015.

[27] X.-L. Zhi, X.-X. Jiang, and A.-M. Sha, "Pavement subbase course stress by vibrating compaction on course," *Journal of Chang'an University (Natural Science Edition)*, vol. 23, no. 3, pp. 33–36, 2003.

[28] P. H. Shen and S. S. Lin, "Overall dynamics analysis and test of compaction system in double excited mode," *Vibration and Shock*, vol. 36, no. 11, pp. 232–241, 2017.

[29] G. H. Li, *Bridge Structure Stability and Vibration*, China Railway Publishing House, 2nd edition, 1996.

[30] K. Z. Lei, "Calculation of bending moment of a single moving concentrated load acting on a continuous beam," *Shanxi Architecture*, vol. 37, no. 20, pp. 51-52, 2011.